Materials Science & Engineering A 563 (2013) 168–176

Contents lists available at SciVerse ScienceDirect

Materials Science & Engineering A

journal homepage: www.elsevier.com/locate/msea

Microstructure evolution during warm working of Ti–5Al–5Mo–5V–1Cr–1Fe at 600 and 800 °C

S.V. Zherebtsov [a,*], M.A. Murzinova [b], M.V. Klimova [a], G.A. Salishchev [a], A.A. Popov [c], S.L. Semiatin [d]

[a] Laboratory of Bulk Nanostructured Materials, Belgorod State University, Pobeda-85, Belgorod 308015, Russia
[b] Institute for Metals Superplasticity Problems, Khalturina-39, Ufa 450001, Russia
[c] Ural Federal University, Mira-19, Ekaterinburg 620002, Russia
[d] Air Force Research Laboratory, Materials and Manufacturing Directorate, AFRL/RXLM, Wright-Patterson Air Force Base, OH 45433-7817, USA

ARTICLE INFO

Article history:
Received 31 July 2012
Received in revised form
22 October 2012
Accepted 9 November 2012
Available online 20 November 2012

Keywords:
Titanium alloys
Thermomechanical processing
Microstructure refinement
Speroidization
Precipitation

ABSTRACT

Microstructure evolution during compression to the true height strain 0.29, 0.69, or 1.2 at 600 and 800 °C of the β-rich titanium alloy Ti–5Al–5Mo–5V–1Cr–1Fe (VT22) with an initial lamellar microstructure was established using scanning and transmission electron microscopy. It was found that microstructure evolution at both temperatures was controlled primarily by substructure evolution within the β phase. At 800 °C, extensive recovery within the β phase resulted in the formation of a stable structure comprising subgrains ~1.5 μm in diameter. During deformation at this temperature, lamellae of the α phase fragmented via a boundary-grooving mechanism. Due to the sluggish diffusion kinetics, however, spheroidization at 800 °C was incomplete. At the lower processing temperature, recovery processes within the β phase were much slower, leading to greater refinement of the β matrix. The decomposition of the metastable β phase during warm working, gave rise to very fine α-lath precipitates, which resulted in the formation of an ultrafine microstructure with a grain size of 0.5 μm.

1. Introduction

Two-phase α/β titanium alloys exhibit a broad range of microstructures such as the lamellar one which forms as the result of β→α+β transformation during cooling from the high-temperature single-phase β region. Such a microstructure has good creep and fatigue-crack-growth resistance, but low ductility [1]. A better balance of strength and ductility is obtained with a globular-(equiaxed-) α microstructure [1]. In the ultrafine grained (UFG) condition (grain size~100–500 nm), superior mechanical properties are achieved [2,3].

The globular microstructure in two-phase titanium alloys is produced via hot deformation of a starting lamellar microstructure in the $\alpha+\beta$ phase field. A refinement in microstructure can be realized by decreasing the deformation temperature. For example, multi-axial isothermal forging of Ti–6Al–4V at 550 °C [4] has been shown to result in a homogeneous, globular microstructure with a grain/subgrain size of 300 nm.

The mechanisms and kinetics of the spheroidization of lamellar microstructures in α/β titanium alloys such as Ti–6Al–4V have been investigated over a wide range of hot- and warm-working temperatures [5–8]. At high temperatures, spheroidization is often associated with (i) the generation of transverse boundaries within alpha lamellae, (ii) the subsequent formation of grooves associated with the instability of 90° dihedral angles between *interphase* α/β boundaries and *intraphase* α/α boundaries, and (iii) complete lamellar fragmentation by deepening of the grooves from both sides of the α lamellae. The mechanism of fragmentation via boundary grooving may be applicable to the plate-like β phase as well. However, the kinetics are likely slower for fragmenting β lamellae because diffusion of solutes through the α-phase (which controls the grooving kinetics of the β-layers) is relatively slow [9]. Lamella thickness, deformation temperature, and the nature of the intragranular and α/β interfaces (e.g., boundary energy) are the main factors influencing the mechanism and kinetics of spheroidization [8,10,11]. Hence, the kinetics of recovery, recrystallization, shear band formation, etc. within α lamellae strongly affect fragmentation [6]. In addition, the evolution of (semi)coherent α/β interphase boundaries into noncoherent ones during deformation [11] may enhance diffusion along the interfaces [8,12] but make slip transfer more difficult.

The mechanisms and kinetics of deformation and spheroidization of lamellar microstructures in titanium alloys with large amounts of the β-stabilizing elements (and hence β phase at a given processing temperature) have been studied to a lesser degree than for Ti–6Al–4V. For example, the equilibrium fraction of β phase in Ti–5Al–5Mo–5V–1Cr–1Fe (i.e., the Russian alloy VT22) is ~0.5 at room temperature [13]. Differences in the α/β

* Corresponding author. Tel.: +7 4722 585416; fax: +7 4722 585415.
E-mail address: ser_z@mail.ru (S.V. Zherebtsov).

0921-5093/$ - see front matter © 2012 Elsevier B.V. All rights reserved.
http://dx.doi.org/10.1016/j.msea.2012.11.042

phase ratio of β-rich alloys can modify the specific features of microstructure evolution especially at warm-working temperatures due to differences in strain partitioning between the softer β phase and the harder α-phase. Moreover, the sluggishness of the decomposition of solute-enriched β phase can influence microstructure evolution significantly [14–17]. The objective of the present work, therefore, was to elucidate the mechanisms of microstructure evolution in a typical β-rich alloy (VT22) during warm working and thus establish the feasibility of achieving a UFG microstructure by warm working.

2. Materials and procedures

The program material was VT22 with a composition (in wt%) of 5.1Al–4.9Mo–5.4V–1.0Cr–1.0Fe–0.08Si–0.1O. It was received in the form of a 25-mm-diameter hot-rolled bar with a β-transus temperature (at which $\alpha+\beta\rightarrow\beta$) of 860 °C. To develop a lamellar microstructure, the bar was beta annealed at 975 °C for 30 min, cooled rapidly to 820 °C and soaked for 2 h, cooled to 750 °C and soaked for 8 h, and finally water quenched. This treatment produced a colony microstructure comprising α lamellae within a matrix of β phase (Fig. 1a).

Microstructure evolution during warm working was established using isothermal compression testing. For this purpose, cylindrical compression samples measuring 8-mm diameter × 12-mm height were machined from the heat-treated bar. Specimens were soaked 15 min prior to deformation and compressed isothermally in air at 800 or 600 °C in a Schenk mechanical-testing system at a constant crosshead speed corresponding to an initial strain rate of $10^{-3}\,s^{-1}$. To decrease friction between the surfaces of the dies and the specimen, graphite grease was used. The imposed *average* true height strain ε was 0.29, 0.69, or 1.2 (corresponding to 25%, 50%, or 70%. height reduction, respectively). The local effective strains at the center of the samples (at which all metallographic measurements and observations were made) were larger than the average sample deformation, however. For example, in Ref. [18], the maximum local effective strain was invariably found at the center of the deformed specimen and was estimated to be 0.49, 1.1, or 1.5 for material upset to an average true height strain of 0.3, 0.6, or 0.9, respectively. In the sections that follow, strain values are reported as *average* true height strain. However, it should be remembered that the *local effective* strain at the center of specimens was noticeably higher. Each specimen was water quenched immediately after compression.

Stress–strain curves were derived from measured pressure–height reduction plots assuming uniform deformation. Because the axial true strain rate increased by a factor of three during compression at the constant crosshead speed (to a 3:1 height reduction), the flow curves were corrected in an approximate fashion to a constant strain rate by multiplying each flow stress datum by a factor equal to $(h/h_o)^m$, in which h and h_o are the instantaneous and original sample height, respectively, and m (≈ 0.25) is the strain rate sensitivity.

Following deformation, axial sections were prepared for the determination of the microstructure in the central portion of each specimen using a JEOL JSM-840 or FEI Quanta 600 FEG scanning electron microscope (SEM) and a JEOL JEM-2100FX transmission electron microscope (TEM). X-ray investigation was performed using an ARL X'TRA (Thermo) diffractometer with Cu-Kα radiation (40 kV, 30 mA). X-ray patterns were collected in the range $2\theta=10°$–$90°$ with the step size of 0.02°. The examined area was ~0.5 mm^2 for each sample. Quantitative phase analysis was made by the Rietveld method [19] using the PowderCell software. The volume fraction of the primary-α phase in some selected specimens was also evaluated by metallographic analysis.

The spheroidized fraction of the α lamellae was determined based on an aspect ratio $k=l/b<2$, in which l and b denote the length and thickness, respectively, of remnant α lamellae/particles. For this purpose, a total area of approximately 0.8 mm^2 lying in the most heavily deformed part of each specimen was examined for each deformation condition. The error for each measurement was estimated to be less than 10% with an 80% confidence interval.

Bulk specimens with an ultrafine grain microstructure were produced by multi-axial forging (MF) under isothermal conditions [4]. For this purpose, specimens water quenched following beta annealing were worked in the temperature interval of 700–550 °C using a 6400-kN hydraulic press equipped with isothermal-forging tooling. The nominal strain rate in these trials was also $\sim 10^{-3}\,s^{-1}$.

3. Results and discussion

3.1. Initial microstructure

The microstructure of the program alloy in the as-heat-treated condition (i.e., after water quenching from 750 °C) consisted of lamellar-α colonies within prior β grains (Fig. 1a); the fraction of the α phase was 0.28 ± 0.02. The sizes of the α colonies and β grains were ~30 μm and ~230 μm, respectively, and the thickness of the α lamellae was ~1.1 μm. The α lamellae were heterogeneously distributed within the β matrix; the average distance between α lamellae was 2.5 μm however a number of relatively large areas of the β matrix (spanning ~10–20 μm in extent) free of α precipitation was observed (some of them are marked by arrows Fig. 1a).

TEM images revealed a complex structure of the phases after the heat treatement (Fig. 1b–d). For example, many alternating, thin gray and light lamellae with distinct straight boundaries were observed within the β matrix between the thicker α lamellae (Fig. 1b, c). Each of these internal lamellae consists of very thin laths laying at an angle of 50°–70° to the lamella boundaries (Fig. 1c). Many of the lamellae were parallel to each other, but some intersected each other. Neighboring parallel lamellae had no detectable difference in crystallographic orientation. The specific contrast on the TEM image of the lamellae boundaries implies the presence of local stresses [20]. However, the overall dislocation density in the β phase was very low.

In Ref. [21], the formation of fine lamellae within the layers of the β matrix of this alloy was ascribed to the precipitation of a body-centered-tetragonal τ phase via a shear transformation. A diffraction pattern from the β phase (inset in Fig. 1c) did not show any other phases. Nevertheless, the presence of "bands" between reflections of the β phase may imply the presence of areas of short-range order with a structure varying somewhat from the matrix.

In the thick α-phase lamellae, a high dislocation density and many twins with a thickness of 40–50 nm were noted (Fig. 1d). The α/β interphase boundaries were sharp and narrow without any visible signs of stresses in contrast to previous results for alloys such as Ti–6Al–4V [6]. This observation may imply a high level of coherency between the α lamellae and the β matrix.

The microstructures of test samples prior to deformation (i.e., preheated at 800 or 600 °C for 15 min and then water quenched) are summarized in Fig. 2. Preheating at 800 °C did not lead to a noticeable change in microstructure (Fig. 2a). On the other hand, annealing at 600 °C resulted in the formation of acicular secondary-α laths in some areas of the β matrix which had previously been devoid of coarse α lamellae (Fig. 2b). At high magnification, the secondary-α laths were noted to comprise a dense Widmanstatten structure located in the central parts of large

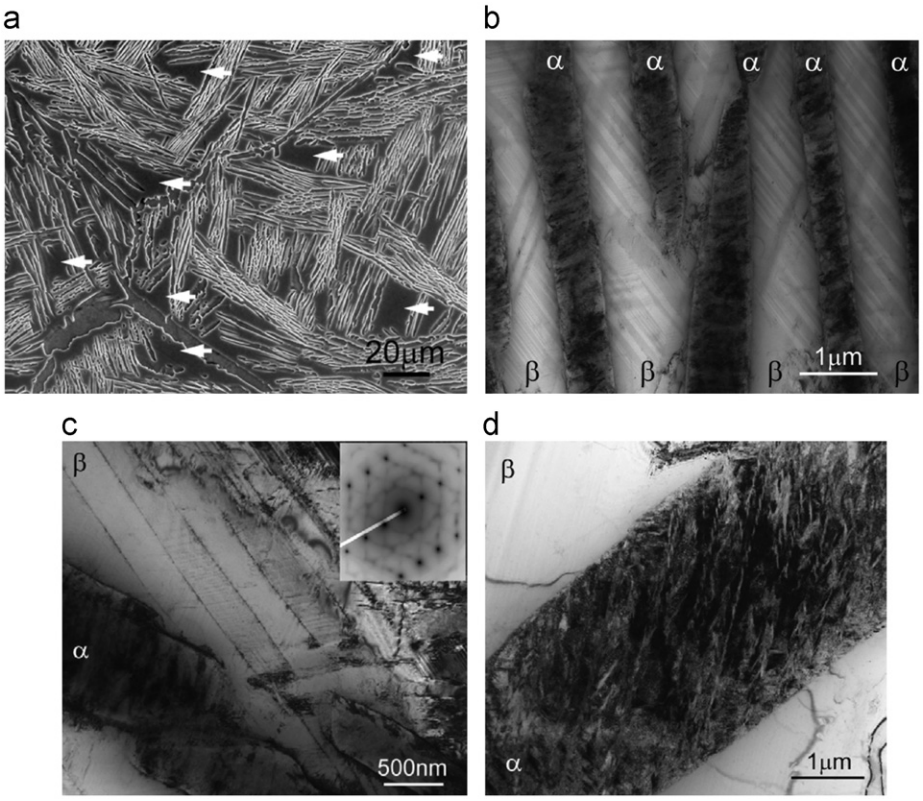

Fig. 1. The initial (heat-treated) microstructure of the Ti–5Al–5Mo–5V–1Cr–1Fe program alloy: (a) SEM, (b–d) TEM.

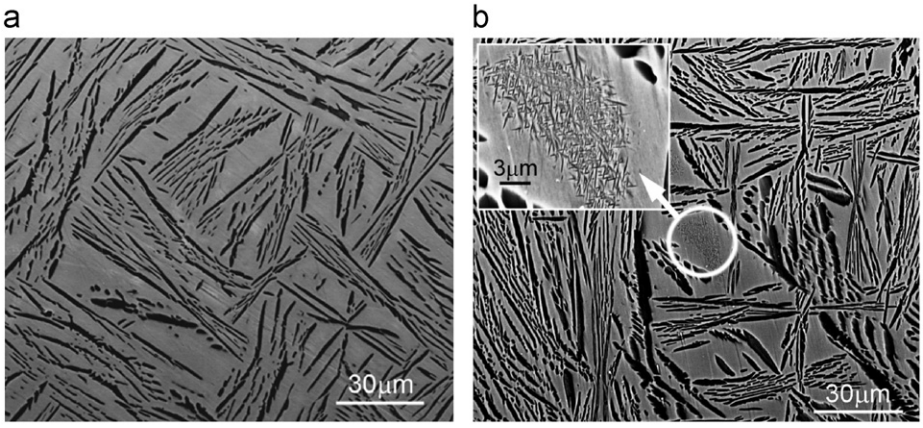

Fig. 2. SEM micrographs of the microstructure developed in Ti–5Al–5Mo–5V–1Cr–1Fe during preheating for 15 min (followed by water quenching) at (a) 800 °C or (b) 600 °C. The inset in (b) illustrates the decomposition of the β phase at higher magnification.

areas of the β matrix surrounded by coarse, lamellar α. The thickness of these secondary-α laths did not exceed 100 nm. It is apparent that the precipitation of the α phase at 600 °C was associated with the metastability of the β-phase generated during quenching from 750 °C to produce the initial condition. In related prior work [14,22], the precipitation of very small, elongated secondary-α laths *during annealing* at 650 °C of Ti–5Al–5Mo–5V–1Cr–1Fe previously water quenched from the β phase field had also been reported.

3.2. Microstructure evolution during deformation at 800 and 600 °C

The main features of microstructure evolution during compression at both 800 and 600 °C consisted of thinning/elongation of the β grains and rotation of the α lamellae toward the metal-flow direction (Fig. 3). Bent α lamellae and regions of localized shear were observed in those α colonies for which the lamellae were initially close to being *parallel* to the compression axis (some examples are shown by dashed lines in Fig. 3a, b and d). Such bending and localized shear banding tended to rotate portions of α lamellae, thereby leading to the activation of new slip systems during deformation. Local bending of lamellae was also observed in the vicinity of colony or grain boundaries due to deformation incompatibility. Those colonies in which the lamellae were initially aligned with the metal flow direction (i.e., perpendicular to the compression axis) underwent little morphological change during deformation. With increasing strain, almost all of the lamellae became aligned with the metal-flow direction at both temperatures. A microstructure comprising mainly fragmented, lamellar-α phase in the β-matrix was observed after a strain $\varepsilon = 1.2$ (Fig. 3e, f).

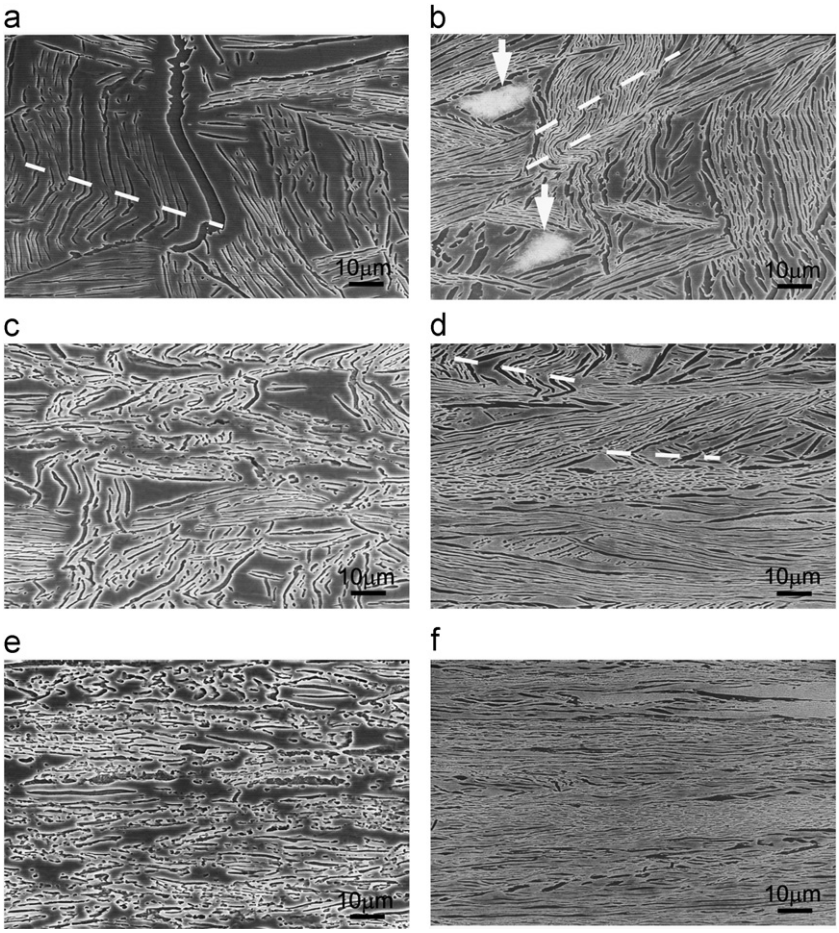

Fig. 3. SEM micrographs of Ti–5Al–5Mo–5V–1Cr–1Fe following compression at (a, c, e) 800 °C or (b, d, f) 600 °C and a nominal strain rate 10^{-3} s^{-1} to a true average height strain of (a, b) 0.29, (c, d) 0.69, or (e, f) 1.2. In (b), areas of secondary-α precipitation are shown with arrows. The compression axis is vertical in all micrographs.

The size of individual globular-α fragments at this level of deformation was 1–1.5 μm at 800 °C and ~0.5 μm at 600 °C.

Small regions of acicular secondary-α were seen in the SEM micrographs from samples deformed to a strain of 0.29 at 600 °C (arrows in Fig. 3b). However, such regions disappeared with strain and were not observed at all for $\varepsilon > 0.69$.

TEM investigation provided more detailed insight into microstructure evolution during warm working. After a strain of 0.29 at 800 °C, for instance, there was little change in microstructure in comparison with the initial condition. However, there was an increase in dislocation density, and subboundaries with a misorientation of 1°–2° (arrow in Fig. 4a) were observed in the β-phase. These subboundaries were found primarily in those areas in which the α lamellae were closely-spaced. A similar effect has been reported previously for the β-rich alloy Ti–10V–2Fe–3Al [23].

Similar to the initial condition, alternating thin gray and light lamellae were observed in the β phase after $\varepsilon = 0.29$ at 800 °C (parallel to the arrow in Fig. 4a). During deformation, the boundaries of some of these fine lamellae became decorated with dislocations. However, the subboundaries formed within the β layers during deformation did not form jogs nor bend when intersecting with the fine gray/light internal lamellae. This fact also supports the conclusion that the fine internal lamellae formed during rapid cooling *following* deformation (via the shear β→τ transformation [21]) in a manner similar to their development during the initial heat treatment of the material.

After a strain of 0.69 or 1.2 at 800 °C, subgrains of a size ~1.5 μm in diameter with low-to-medium misorientation were observed in some areas of the β-phase matrix layers (Fig. 4b). However, the dislocation density increased and substructure developed slowly in the β phase and mainly in those areas in which lamellae of the α-phase were present.

In contrast to the behavior of the β layers, the microstructure of the α lamellae changed relatively little during deformation at 800 °C. By a strain of 0.69, a few transverse boundaries and local curvature (grooving) of the lamellae interfaces had developed. After $\varepsilon = 1.2$ some of α lamellae had divided into separate elongated fragments (Fig. 4b). In addition, the α/β interphase boundaries had become irregular and less sharp in comparison with the initial condition, most likely due to the trapping of lattice dislocations.

A decrease in deformation temperature to 600 °C resulted in a greater increase in dislocation density in the β phase in comparison with deformation at 800 °C. Subgrains/cells with an irregular shape and a size of ~1 μm or less were formed within the β-phase layers (Fig. 5a). In those areas of the β layers in which substructure was absent, fine gray and light lamellae were observed but their number was less than in the initial heat-treated condition.

Deformation to a strain of 0.69 at 600 °C led to quite sluggish microstructure evolution in the α lamellae. In fact, the α lamella retained their original integrity without fragmentation by transverse boundaries/grooving even in regions subjected to localized kinking to an angle of the order of 90° (Fig. 5b).

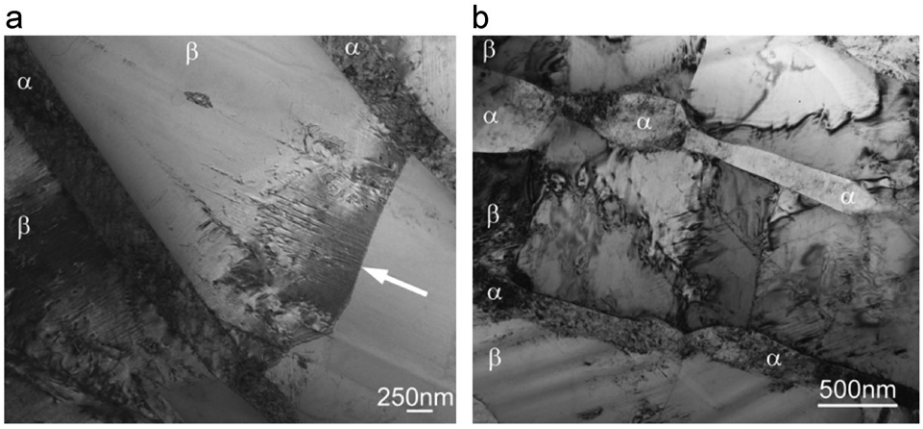

Fig. 4. Bright-field TEM images of the microstructure developed in Ti–5Al–5Mo–5V 81Cr–1Fe during deformation at 800 °C to a height strain of (a) 0.29 or (b) 1.2.

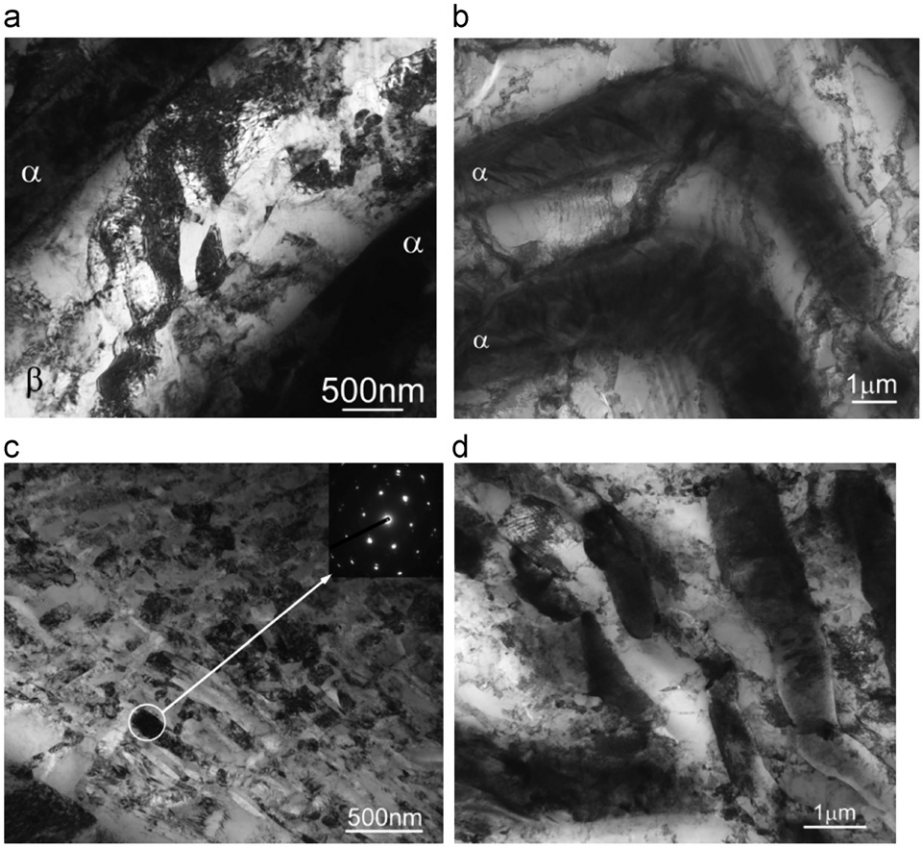

Fig. 5. Bright-field TEM images of the microstructure developed in Ti–5Al–5Mo–5V–1Cr–1Fe during deformation at 600 °C to a high strain of (a–c) 0.69 or (d) 1.2.

An increase in height strain to 1.2 at 600 °C resulted in the formation of subgrains with low-to-medium misorientation in the β phase. Some α phase lamellae had fragmented by this level of deformation, and the corresponding fragments had shifted relative to each other. However, spheroidization developed very slowly, and thus the lamellar morphology of the α phase generally survived even after such a large strain (Fig. 5d).

As mentioned in Section 3.1, an important feature of microstructure evolution at 600 °C was the precipitation of acicular secondary α during preheating *prior* to deformation. As a result, a very fine microstructure consisting of 70–100-nm-diameter particles was observed by TEM in some areas of the β-phase layers at $\varepsilon > 0.29$ (Fig. 5c). These particles were typically elongated with an aspect ratio (length/width) $k \geq 2$. The fraction of such fine-grained microstructure increased with strain. Diffraction patterns for these particles (inset in Fig. 5c) indicated that they were hcp α phase.

The results of the quantitative X-ray analysis indicated that the precipitation of secondary-α particles began during preheating (Fig. 2b) and continued during deformation at 600 °C. Specifically, the overall fraction of the α phase *increased* from 0.28 in the initial condition (i.e., WQ'ed from 750 °C) to 0.38 after the 15-min soak at 600 °C and ~0.45 during further deformation at this temperature. By contrast, the fraction of the α phase at 800 °C *decreased* from 0.28 to 0.24 during preheating and to ~0.19 during deformation (to a strain level of 1.2; Fig. 6). At both temperatures, the largest change in the phase fraction *during* deformation (either decrease or increase) was found in the strain interval between 0 and 0.29.

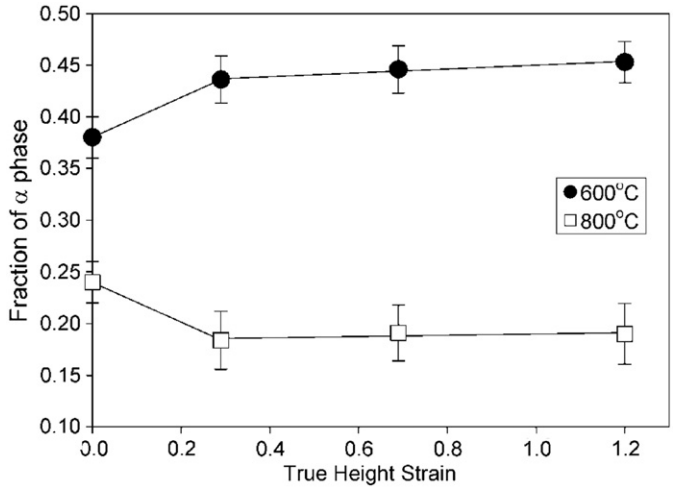

Fig. 6. Dependence of the fraction of α phase in Ti-5Al–5Mo–5V–1Cr–1Fe on strain during deformation at 800 and 600 °C. The data for $\varepsilon=0$ correspond to a 15-min soak at the respective temperature followed by WQ.

The similarity in the thickness of the secondary-α laths formed during soaking prior to deformation and the size of the α particles developed during deformation at 600 °C suggested that the formation of small globular grains was the result of dynamic spheroidization due to particle fragmentation. The retention of an aspect ratio $k \geq 2$ for many of the particles also underlies the fact that they may have nucleated as fine laths and been only partially fragmented during subsequent deformation. On the other hand, some of the more equiaxed particles may have been nucleated in a spheroidal shape. This morphology was promoted perhaps by heterogeneous, dynamic precipitation on lattice defects (e.g., dislocations) and concurrent enhanced (pipe) diffusion processes leading to a minimization in the surface energy of such particles.

3.3. Flow behavior and kinetics of microstructure evolution

At both temperatures, the strain-rate corrected flow curves exhibited an initial hardening transient, a peak flow stress at $\varepsilon \approx 0.04$, and then flow softening (Fig. 7a). The softening was relatively marked at both temperatures, resulting in a reduction in flow stress *relative to the peak value* of either 50% or 38% after an average height strain of 1.2 at 800 or 600 °C, respectively. Such behavior in single-phase metallic materials is often associated with discontinuous dynamic recrystallization [24]. For two-phase titanium alloys, on the other hand, mechanisms such as slip transfer [10], dynamic fragmentation [23], and texture softening have been suggested. An analysis of the results in [23] reveals that the fractional softening of Ti–10V–2Fe–3Al with a Widmanstatten-α preform microstructure was of the order of 50% for a strain of ~0.7 in the temperature range between 760 and 790 °C and a strain rate of $10^{-3}\,s^{-1}$. The slightly lower level of fractional softening found at 600 °C in the present work may be due to the small amount of dynamic precipitation of fine α phase within the β layers (noted above) which would provide an increment of strengthening. Although most of the dynamic precipitation occurred at small strains at which the measured flow softening rate was greatest, the effect would be expected to be small because the preponderance of secondary-α precipitation occurred during preheating prior to deformation at this temperature.

The kinetics of microstructure evolution were quantified in terms of the average length, thickness and inclination angle of α lamellae and the fraction of globularized-α phase. At both temperatures, the inclination of the α lamellae relative to the compression direction increased with strain (Fig. 7b). The rate of lamellar rotation decreased with strain and increased with a decrease in temperature. The average inclination angle after a height strain of 1.2 was ~70° and ~80° at 800 and 600 °C, respectively.

Although the α lamellae showed a greater rotation during the same strain interval over which flow softening occurred, a relationship between such rotation (and the associated changes in the texture/average Taylor factor of the α phase) and the shape of the stress–strain curves was not apparent. Such a relationship may be expected to be weak especially since the bulk of the imposed deformation was accommodated by the bcc β phase, which tends to exhibit limited plastic anisotropy compared to the hcp α phase in titanium alloys. Hence, as noted above, it is likely that the observed flow softening may be ascribed primarily to slip transfer [10] and fragmentation of the β matrix [23]. The latter effect would reduce the constraint imposed on the deformation of β and hence the stress required to bring about its deformation.

The apparent length of α lamellae during deformation at 800 °C steadily decreased with strain (Fig. 7c). This behavior mirrors typical changes associated with dynamic fragmentation and spheroidization of α lamellae [23]. At the lower temperature (600 °C), the length of α lamellae did not change until $\varepsilon \sim 0.69$, but decreased rather rapidly at larger strain almost attaining the value of the lamella length at 800 °C after $\varepsilon=1.2$. Despite the decrease in average apparent length of the lamellae, the maximum fraction of globular-α particles (with an aspect ratio of 2 or less) after a height reduction of 1.2 was only ~15% at 800 °C and ~3% at 600 °C (Fig. 7d).

In contrast to the length, the apparent thickness of α lamellae at 800 °C decreased considerably during deformation until $\varepsilon=0.29$ and then did not change markedly, whereas it decreased steadily during the overall strain interval at 600 °C (Fig. 7e). The thinning of lamellae during deformation of Ti–6Al–4V was discussed in Refs. [6,7]. In these previous efforts, thinning observations were interpreted in the context of three main factors: homogeneous strain itself, a so-called "stereological effect" (apparent decrease in thickness due to rotation of lamellae with respect to the cross-section), and strain partitioning between the α and β phases associated with differences in flow stress. The initial, relatively-rapid decrease in α-lamellae thickness during the interval of deformation between 0 and 0.29 at both temperatures is most probably a result of lamellae rotation toward the metal flow direction (i.e., the stereological effect). During further straining at 800 °C, the nearly-constant thickness of the lamellae may be associated with a competition between the stereological effect (which becomes less pronounced with strain) and perhaps a small amount of thickening via the termination–migration mechanism. Strain-induced thinning of lamellae at 800 °C is likely limited due the small volume fraction of the α phase (Fig. 6) and its considerably greater flow stress relative to that of the β matrix. [25]. By contrast, a decrease in temperature to 600 °C substantially increases the fraction of harder α-phase, thereby reducing the degree of strain partitioning. Hence, at the lower temperature, thinning due to strain and the "stereological effect" are surmised to give rise to the behavior in Fig. 7e. At the lower temperature, lamellar coarsening due to termination migration would be expected to be minimal.

Overall, the quantitative and qualitative data on microstructure evolution revealed that the spheroidization of the α-phase during deformation was quite sluggish. Important factors influencing the rate of spheroidization due to the sequential processes of fragmentation and termination migration are the thickness of the lamellae and the temperature of deformation. According to Refs. [5] and [26], the time t_p, to complete fragmentation via grooving is given by the relation

$$t_p = 0.2(d_\alpha)^3/A(m_g)^3, \quad (1)$$

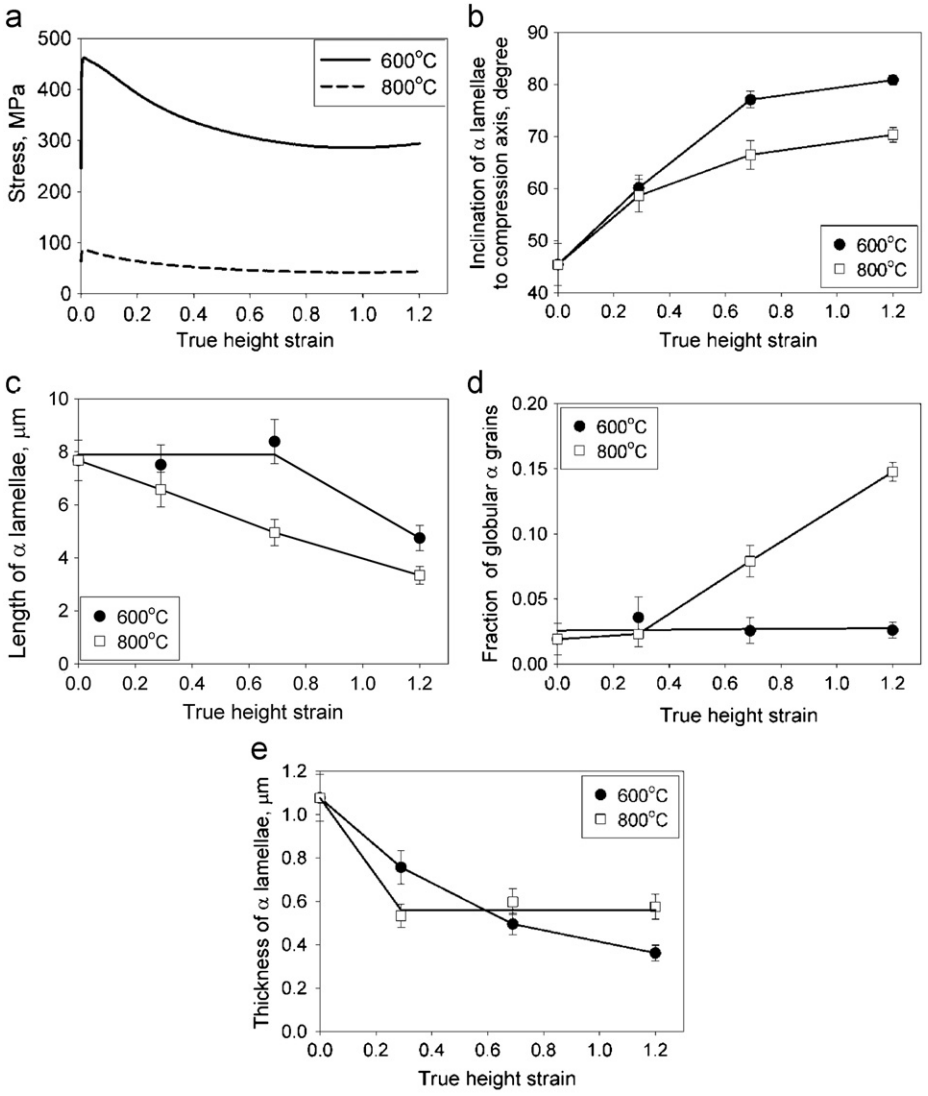

Fig. 7. (a) Flow curves obtained during deformation at 800 and 600 °C and a strain rate of $10^{-3}\,s^{-1}$, (b) Inclination of α lamellae to the compression axis, (c) length of α lamellae, (d) fraction of globular α particles (with aspect ratio $k \le 2$) and (e) thickness of α lamellae as a function of strain for Ti–5Al–5Mo–5V–1Cr–1Fe deformed at 800 and 600 °C.

in which d_α is the thickness of the α lamella, and m_g represents the average slope at the root of the triple point [27]. The coefficient A is given by the equation [5]:

$$A = C_\beta \gamma_{\alpha\beta} V_M D_\beta / R_g T, \quad (2)$$

in which C_β denotes the *equilibrium* concentration (expressed as an atomic fraction) of the rate-limiting solute in the β phase (taken to be Mo for Ti–5Al–5Mo–5V–1Cr–1Fe); $\gamma_{\alpha\beta}$ is the α/β interface energy; V_M is the molar volume of the α platelet material; D_β is the diffusivity of the rate-limiting solute through the β matrix; R_g is the universal gas constant; and T is the absolute temperature. Because neither the α nor the β phase in the program alloy is a terminal solid solution, the term C_β in the expression for the coefficient A should be replaced by the composition factor C_F [5,28]:

$$C_F = C_\beta(1-C_\beta)/(C_\alpha - C_\beta)^2[1+\partial \ln r/\partial \ln C_\beta]. \quad (3)$$

here, C_α is the concentration of the rate-limiting solute in the α phase and the term $[1+\partial \ln r/\partial \ln C_\beta]$ is a thermodynamic factor ($r \equiv$ activity coefficient of solute in the β phase). This composition-factor correction is particularly important for those alloys in which there is only a small composition difference, $C_\beta - C_\alpha$, between the phases, thus leading to a large acceleration of the interfacial-energy-driven process [28].

Input data required to calculate the time t_p needed to complete fragmentation via grooving in Ti–5Al–5Mo–5V–1Cr–1Fe comprise the slope m_g (~0.35), the molar volume of the α platelet material (V_M=10,440 mm^3), and the α/β surface energy, taken here to be $\gamma_{\alpha\beta}$=0.26 J/m^2 per Ref. [11]. The α-lamella thickness, d_α, was set equal to ~1.1 μm at both temperatures (Fig. 7e).

The thermodynamic factor for molybdenum solutes in β titanium was assumed to be equal to ~1. The composition term (i.e., $C_\beta(1-C_\beta)/(C_\alpha - C_\beta)^2$) at 600 and 800 °C was calculated using version 5 of the Thermo-Calc software (TTTI3 database). The values of C_β for Mo were found to be equal to 0.026 and 0.06 at 800 and 600 °C, respectively; C_α was 0.0024 at 800 °C and 0.0031 at 800 °C. Thus, C_F was calculated as 47 and 17 at 800 and 600 °C, respectively.

The diffusivity of Mo through the β matrix was calculated from the relation $D^\beta_{Mo}(\mu m/s) = 52{,}500\exp\{-18{,}520/T(K)\}$ in Ref. [29], thus yielding a diffusivity of 3.2×10^{-5} $\mu m^2/s$ at 600 °C and 0.0017 $\mu m^2/s$ at 800 °C. However, these diffusivities are representative of solute transport through an *annealed* (unworked) β matrix. At warm processing temperatures, on the other hand,

substantial dislocation substructure from concurrent warm working is likely present in the β phase, and thus kinetics due to pipe diffusion are enhanced. In several earlier works, the relative increase in diffusivity due to substructure developed during *prior* warm working was assumed to be of the order of a factor of 10 (e.g.[5,6]), thus leading to Mo diffusivities of 3.2×10^{-4} μm^2/s at 600 °C and 0.017 μm^2/s at 800 °C. Substituting these values of D and the other material and geometry parameters into Eqs. (1) and (2) gives the time necessary to complete the boundary-grooving process as ~7.2 and ~850 h at 800 and 600 °C, respectively. Both of these times are substantially longer than the total time for the present experiments, i.e., ~300 s for an imposed strain of 1.2 at a nominal strain rate of 10^{-3} s^{-1}.

If the values of diffusivity were yet higher by perhaps another factor of 10 due to the fact that deformation was concurrent, the predicted times would still be relatively long, i.e., 0.72 h and 85 h at 800 and 600 °C, respectively, compared to the duration of the compression experiments. However, if the calculations are based on the platelet thickness near the end of the experiments (at which the stereological effect is eliminated), i.e., 0.55 μm (Fig. 7e), the predicted fragmentation times are reduced by a factor of $8[(1.1/0.55)^3]$, thus yielding values of 325 s and 10.5 h. The former time (for tests at 800 °C) is comparable to the duration of the experiment, but the latter (for 600 °C) is much greater. Such comparisons thus provide a plausible explanation for the modest or very limited amount of dynamic spheroidization that was observed at the higher and lower test temperatures, respectively (Fig. 7d). The calculations also appear to suggest that the observed reduction in platelet length with strain at the lower temperature (Fig. 7c) may be due to platelet fracture as opposed to fragmentation associated with the boundary-grooving process per se.

The relatively small amounts of dynamic spheroidization and the absence of platelet thickening (Fig. 7d, e) also suggest that minimal termination migration occurred. Such observations can be ascribed to the low temperatures and typical findings that termination migration to complete spheroidization typically requires an order of magnitude more time than platelet fragmentation [27].

Because t_p varies as the cube of the platelet thickness (Eq. (1)), microstructures with much thinner secondary-α laths (formed at the lower warm-working temperature) should fragment much more rapidly than those with thick lamellae. As a result, the very thin secondary α at the lower test temperature transformed readily from an acicular to globular shape.

3.4. Formation of a UFG structure

The present data and results described in Refs. [16] suggest that the instability of the β phase can be used for microstructure refinement during deformation at low (warm-working) temperatures. Two main conditions should be fulfilled for the utilization of this approach: (i) A high degree of supersaturation/β-matrix metastability should be generated via water quenching from the β phase field, and (ii) High levels of strain should be imposed. With regard to the second prerequisite, an almost unlimited level of deformation can be imposed by isothermal MF [4]. In the present work, warm working of Ti–5Al–5Mo–5V–1Cr–1Fe water quenched from the β phase field in the temperature interval of 700–550 °C resulted in formation of a very fine microstructure with an average grain size less than 0.5 μm. However, the microstructure was not completely homogeneous (Fig. 8); areas with equiaxed grains ~0.5 μm in size and regions with lamellae ~100–200 nm thick were observed. Some of the lamellae had started to transform into globular grains; the size of these grains was approximately equal to the thickness of the lamellae.

Because MF was performed at decreasing temperatures from 700→550 °C, the presence of the two types of microstructures

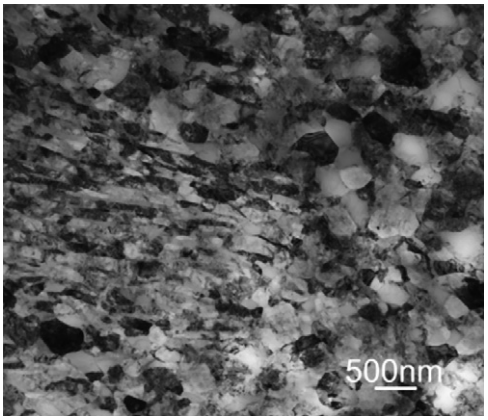

Fig. 8. Bright-field TEM image of the microstructure developed in Ti–5Al–5Mo–5V–1Cr–1Fe after isothermal MF at 700–550 °C.

was ascribed to the specific temperatures of their formation. In particular, the α particles precipitated at higher temperature should be thicker than those developed at lower temperatures. Hence, decomposition of the β phase followed by dynamic spheroidization and coarsening of α particles led to the formation of the coarser globular grains during deformation at higher temperatures (~700 °C). The subsequent decrease in the isothermal forging temperature to 600 and then 550 °C led to further instability of the β phase and resulted in the precipitation of additional α laths which were only partially spheroidized during deformation. An increase in strain and a decrease in the temperature interval of MF would be expected to increase the homogeneity of the UFG microstructure.

4. Conclusions

Microstructure evolution during warm working of the beta-annealed, β-rich titanium alloy Ti–5Al–5Mo–5V–1Cr–1Fe is primarily controlled by processes within the bcc β matrix. At 800 °C, dynamic recovery and subgrain formation occur within the β phase. In regions of the β phase in which deformation is constrained (by nearby α lamellae or grain boundaries), the extent of substructure formation is higher. Due to its relatively small volume fraction (~0.19 at 800 °C), the α phase has a weak effect on microstructure evolution. Lamellae of the α phase fragment during deformation via the classical boundary-grooving mechanism. Full spheroidization via termination migration cannot be completed dynamically due to sluggish diffusion kinetics.

A decrease in deformation temperature to 600 °C retards the dynamic recovery processes in the β phase resulting in more extensive refinement of the matrix. Concurrently, the larger fraction of the α phase promotes the formation of new high-angle boundaries. However, due to the non-uniform distribution of the coarse α lamellae in the β matrix, microstructure refinement occurs quite heterogeneously.

Decomposition of the metastable β phase and the formation of very fine α-particles can be considered as a method to produce an ultrafine grain microstructure in Ti–5Al–5Mo–5V–1Cr–1Fe. In this regard, decomposition of the β matrix occurs first in those areas which are devoid of α phase, i.e., in those areas where high-angle boundaries form slowly. Changes in the loading direction during multi-axis forging and a gradual decrease in the deformation temperature accelerate β-phase decomposition throughout different/new areas of the matrix leading to more homogeneous microstructure refinement.

Acknowledgment

This work was supported by the Federal Agency for Education, Russia; Grant #14.A18.21.1637.

References

[1] C. Leyens, M. Peters (Eds.), Titanium and Titanium Alloys: Fundamentals and Applications, Wiley-VCH Verlag GmbH, Weinheim, 2003.
[2] R.Z. Valiev, R.K. Islamgaliev, I.V. Alexandrov, Prog. Mater. Sci. 45 (2000) 103–189.
[3] M.A. Meyers, A. Mishra, D.J. Benson, Prog. Mater. Sci. 51 (2006) 427–556.
[4] S.V. Zherebtsov, G.A. Salishchev, R.M. Galeyev, O.R. Valiakhmetov, S.Yu. Mironov, S.L. Semiatin, Scr. Mater. 51 (2004) 1147–1151.
[5] S.L. Semiatin, D.U. Furrer, in: D.U. Furrer, S.L. Semiatin (Eds.), ASM Handbook of Fundamentals of Modeling for Metals Processing, vol. 22, ASM International, Materials Park, OH, 2009, pp. 522–535.
[6] S. Zherebtsov, M. Murzinova, G. Salishchev, S.L. Semiatin, Acta Mater. 59 (2011) 4138–4150.
[7] S. Mironov, M. Murzinova, S. Zherebtsov, G.A. Salishchev, S.L. Semiatin, Acta Mater. 57 (2009) 2470–2481.
[8] M.I. Mazurski, G.A. Salishchev, Phys. Status Solidi (B) 188 (1995) 653–658.
[9] Y. Mishin, C. Herzig, Acta Mater. 48 (2000) 589–623.
[10] S.L. Semiatin, T.R. Bieler, Acta Mater. 49 (2001) 3565–3573.
[11] S. Zherebtsov, G. Salishchev, S.L. Semiatin, Philos. Mag. Lett. 90 (2010) 903–914.
[12] C. Herzig, Y. Mishin, in: P. Heitjans, J. Karger (Eds.), Diffusion in Condensed Matter, Springer-Verlag, Berlin, 2005.
[13] A.A. Ilyin, B.A. Kolachev, I.S. Polkin, Titanium Alloys: Composition, Structure, Properties (Reference Book), VILS-MATI, Moscow, 2009.
[14] A.A. Popov, A.G. Illarionov, A.V. Korelin, Met. Sci. Heat Treat. 42 (2000) 348–352.
[15] O.M. Ivasishin, P.E. Markovsky, V.I. Bondarchuk, Titanium 2 (2005) 42–49 (In Russian).
[16] S.V. Zherebtsov, R.M. Galeev, G.A. Salishchev, M.M. Myshlyaev, Phys. Met. Metallogr. 87 (1999) 318–323.
[17] A.A. Ilyin, Mechanism and Kinetics of Phase and Structure Transformation in Titanium Alloys, Nauka, Moscow, 1994.
[18] N. Stefansson, S.L. Semiatin, D. Eylon, Metall. Mater. Trans. A 33 (2002) 3527–3534.
[19] G. Will, Powder Diffraction: The Rietveld method and the Two-Stage Method to Determine and Refine Crystal Structures From Powder Diffraction Data, Springer, Berlin, 2005.
[20] D.B. Williams, C.B. Carter, Transmission Electron Microscopy: A Textbook for Materials Science, Plenum Publishing Corporation, New York, 1996.
[21] A.G. Illarionov, I.V. Narygina, M.S. Karabanalov, S.L. Demakov, A.A. Popov, O.A. Elkina, Phys. Met. Metallogr. 110 (2010) 279–288.
[22] O.M. Ivasishin, P.E. Markovsky, Yu.V. Matviychuk, S.L. Semiatin, Metall. Mater. Trans. A 34 (2003) 147–158.
[23] M. Jackson, R. Dashwood, L. Christodoulou, H. Flower, Metall. Mater. Trans. A 36 (2005) 1317–1327.
[24] F.J. Humphreys, M. Hatherly, Recrystallization and Related Annealing Phenomena, Elsevier, Oxford, 2004.
[25] S.L. Semiatin, F. Montheillet, G. Shen, J.J. Jonas, Metall. Mater. Trans. A 33 (2002) 2719–2727.
[26] W.W. Mullins, J. Appl. Phys. 28 (1957) 333–339.
[27] N. Stefansson, S.L. Semiatin, Metall. Mater. Trans. A 34 (2003) 691–698.
[28] S.L. Semiatin, B.C. Kirby, G.A. Salishchev, Metall. Mater. Trans. A 35 (2004) 2809–2819.
[29] C.H. Park, B. Lee, S.L. Semiatin, C.S. Lee, Mater. Sci. Eng. A 527 (2010) 5203–5211.